

Multiscale Representation Enhanced Temporal Flow Fusion Model for Long-Term Workload Forecasting

Shiyu Wang*

weiming.wsy@antgroup.com
Ant Group
Hangzhou, Zhejiang, China

Zhixuan Chu ✉

The State Key Laboratory of
Blockchain and Data Security,
Zhejiang University
Hangzhou, Zhejiang, China
zhixuanchu@zju.edu.cn

Yinbo Sun*

yinbo.syb@antgroup.com
Ant Group
Hangzhou, Zhejiang, China

Yu Liu

nuoman.ly@antgroup.com
Ant Group
Hangzhou, Zhejiang, China

Yuliang Guo

yuliang.gyl@antgroup.com
Ant Group
Hangzhou, Zhejiang, China

Yang Chen

chenyang.chenyang@antgroup.com
Ant Group
Hangzhou, Zhejiang, China

Huiyang Jian

jianhuiyang.jhy@antgroup.com
Ant Group
Hangzhou, Zhejiang, China

Lintao Ma ✉

lintao.mlt@antgroup.com
Ant Group
Hangzhou, Zhejiang, China

Xingyu Lu

sing.lxy@antgroup.com
Ant Group
Hangzhou, Zhejiang, China

Jun Zhou

jun.zhoujun@antgroup.com
Ant Group
Hangzhou, Zhejiang, China

Abstract

Accurate workload forecasting is critical for efficient resource management in cloud computing systems, enabling effective scheduling and autoscaling. Despite recent advances with transformer-based forecasting models, challenges remain due to the non-stationary, nonlinear characteristics of workload time series and the long-term dependencies. In particular, inconsistent performance between long-term history and near-term forecasts hinders long-range predictions. This paper proposes a novel framework leveraging self-supervised multiscale representation learning to capture both long-term and near-term workload patterns. The long-term history is encoded through multiscale representations while the near-term observations are modeled via temporal flow fusion. These representations of different scales are fused using an attention mechanism and characterized with normalizing flows to handle non-Gaussian/non-linear distributions of time series. Extensive experiments on 9 benchmarks demonstrate superiority over existing methods.

*Both authors contributed equally to this research.

Permission to make digital or hard copies of all or part of this work for personal or classroom use is granted without fee provided that copies are not made or distributed for profit or commercial advantage and that copies bear this notice and the full citation on the first page. Copyrights for components of this work owned by others than the author(s) must be honored. Abstracting with credit is permitted. To copy otherwise, or republish, to post on servers or to redistribute to lists, requires prior specific permission and/or a fee. Request permissions from permissions@acm.org.

CIKM '24, October 21–25, 2024, Boise, ID, USA

© 2024 Copyright held by the owner/author(s). Publication rights licensed to ACM.

ACM ISBN 979-8-4007-0436-9/24/10

<https://doi.org/10.1145/3627673.3680072>

CCS Concepts

• Information systems → Temporal data; • Mathematics of computing → Time series analysis; • Computing methodologies → Neural networks.

Keywords

time series, workload forecasting, multiscale representation

ACM Reference Format:

Shiyu Wang, Zhixuan Chu ✉, Yinbo Sun, Yu Liu, Yuliang Guo, Yang Chen, Huiyang Jian, Lintao Ma ✉, Xingyu Lu, and Jun Zhou. 2024. Multiscale Representation Enhanced Temporal Flow Fusion Model for Long-Term Workload Forecasting. In *Proceedings of the 33rd ACM International Conference on Information and Knowledge Management (CIKM '24)*, October 21–25, 2024, Boise, ID, USA. ACM, New York, NY, USA, 9 pages. <https://doi.org/10.1145/3627673.3680072>

1 Introduction

With the continuous expansion of cloud computing, efficient resource management has become a crucial issue for cloud systems [13, 14, 30, 49]. Accurately predicting future workloads is essential for effective resource scheduling [29, 36]. For microservices systems, request per second (RPS) is their main service capacity metric, which quantifies their workload [20, 40]. Therefore, we achieve workload forecasting for microservices by predicting RPS. In recent years, major cloud service providers have successively launched their own resource scaling service frameworks, such as Google's Autopilot [37], Microsoft's FIRM [34], and Amazon's AWS Autoscaling, which adopt different workload forecasting methods. Autopilot uses ARIMA [1, 28], FIRM uses historical statistical methods, and

AWS adopts DeepAR [38], among others. Especially recently, with the increasing complexity of cloud computing services, there has been widespread attention and research on forecasting long-term workloads time series [2, 17, 20, 25, 27, 42]. Notably, a plethora of transformer-based methods, such as Informer [54], Autoformer [22], Fedformer [55], and PatchTST [31], have emerged in abundance. Notwithstanding, it is imperative to highlight that current research confronts the following challenges due to the complex characteristics of time series:

- **Challenge 1: The multi-periodic, non-stationary, and long-term dependencies.** In long-term forecasting, workloads time series data is usually high-frequency and non-stationary with complex multi-periodic characteristics, such as hourly, daily, and weekly cycles. Furthermore, these data exhibit long-term dependent properties. Hence, capturing the multi-periodic and long-term characteristics of time series data is critical in addressing the challenges of long-term forecasting.
- **Challenge 2: The non-Gaussian/non-linear characteristics of workloads time series that have not been adequately characterized.** Time series data often exhibits non-Gaussian/non-linear distributions, which previous studies have predominantly assumed to be Gaussian. This assumption has made it challenging for these studies to adapt to the real distribution of time series data.
- **Challenge 3: The inconsistency between the long-term history of time series and near-term observations.** The significant fluctuations and changes in time series data often result in inconsistent performance between long-term history and near-term observations. While long-term history exhibits complex multi-periodic characteristics, near-term observations show a rapidly changing trend. Therefore, integrating the characteristics of both long-term history and near-term observations is crucial for accurate long-term forecasting.

Recently, significant progress has been made in representation learning, particularly in the area of self-supervised contrastive learning [3–7, 18]. Harness representation learning to capture the long-term dependency and multi-periodic characteristics of time series data is indeed a potent way. Undoubtedly, this introduces a fresh approach to tackling the aforementioned challenges. Unfettered by the limitations of the original end-to-end model, we can devise a novel learning paradigm for long-term time series forecasting.

In this work, we propose a two-stage framework that consists of a *pretraining representation stage* and a *fusion prediction stage*. During the *pretraining representation stage*, we pre-train a multiscale time series representation model using a contrastive learning method in both time and frequency domains. This model extracts representations of different scales from the long-term history of the time series to characterize long-term dependencies and complex multi-periodic patterns [11]. In the *fusion prediction stage*, a temporal flow fusion model captures the changing trends in near-term observations. The multiscale representations of the long-term history and the nearby observations are fused through a

FusionAttention module employing a multi-head attention mechanism. Furthermore, we use normalizing flow to model the non-Gaussian/non-linear properties of the time series. Our approach produces accurate predictions that capture both long-term patterns and near-term trends.

Our Contributions can be summarized as follows:

- This paper presents a novel long-term workload forecasting framework unifying multiscale time series representation learning and temporal flow fusion modeling to capture both long-term historical patterns and near-term trends. This unified approach leads to superior prediction accuracy.
- We propose an original multiscale representation method applying contrastive learning in time and frequency domains to encode long-term dependencies and multi-periodic patterns from long-term history.
- We conducted extensive experiments on nine benchmarks, and our method achieved consistent state-of-the-art performance. Furthermore, we have conducted large-scale deployment in the real-world as a cornerstone of workload forecasting in the Alipay cloud resource management system.

2 Related Work

Time Series (TS) Forecasting. Due to the immense importance of time series forecasting, various models have been well developed. In recent years, a variety of time series forecasting models, particularly those based on deep learning methods, have become increasingly popular [8, 21, 39, 41, 43, 47, 48, 56]. These models have introduced many novel structures and have outperformed classical models such as ARIMA and VAR. Informer [54] is a prob-sparse self-attention mechanism-based model to enhance the prediction capacity in long-sequence TS forecasting. Autoformer [46] is a decomposition architecture that incorporates the series decomposition block as an inner operator. Fedformer [55] is a decomposed Transformer architecture that utilizes a mixture of experts for seasonal-trend decomposition and is enhanced with frequency information. Non-stationary Transformers [26] is to enhance the predictability of time series while maximizing the model’s predictive capacity. PatchTST [31] is an effective design of Transformer-based models for time series forecasting tasks by introducing two key components: patching and channel-independent structure.

Time Series (TS) Representation. Representation learning has recently achieved great success in advancing TS research by characterizing the long temporal dependencies and complex periodicity based on the contrastive method [12, 16, 19, 52, 53]. TS2Vec [50] was recently proposed as a universal framework for learning TS representations by performing contrastive learning in a hierarchical loss over augmented context views. COST [45] proposed a new TS representation learning framework for long-sequence TS forecasting, which applies contrastive learning methods to learn disentangled seasonal-trend representations. TST [51] is a newly developed framework that utilizes the transformer encoder architecture for multivariate time series representation learning. LaST [44] utilizes variational inference to separate seasonal-trend representations

in the latent space. TimeMAE [9] is a novel self-supervised paradigm for learning transferrable time series representations based on transformer networks

Normalizing flow. Normalizing flows(NF) [23], which learn a distribution by transforming the data to samples from a tractable distribution where both sampling and density estimation can be efficient and exact, have been proven to be powerful density approximations [32, 33, 35]. NF are invertible neural networks that typically transform isotropic Gaussians to fit a more complex data distribution [23]. They map from \mathbb{R}^D to \mathbb{R}^D such that densities p_Y on the input space $Y \in \mathbb{R}^D$ are transformed into some tractable distribution p_Z (e.g., an isotropic Gaussian) on space $Z \in \mathbb{R}^D$. This mapping function, $f : Y \rightarrow Z$, and inverse mapping function, $f^{-1} : Z \rightarrow Y$ is composed of a sequence of bijections or invertible functions, and we can express the target distribution densities $p_Y(y)$ by

$$p_Y(y) = p_Z(z) \left| \det \left(\frac{\partial f(y)}{\partial y} \right) \right|, \quad (1)$$

where $\partial f(y)/\partial y$ is the Jacobian of f at y .

For mapping function f , we can employ RealNVP [15] architecture, which is a neural network composed of a series of parametrized invertible transformations with a lower triangular Jacobian structure and vector component permutations in order to capture complex dependencies. It leaves the part of its inputs unchanged and transforms the other part via functions of the un-transformed variables (with superscript denoting the coordinate indices)

$$\begin{cases} y^{1:d} = x^{1:d} \\ y^{d+1:D} = x^{d+1:D} \odot \exp(s(x)^{1:d} + t(x^{1:d})) \end{cases}, \quad (2)$$

where \odot is an element wise product, $s()$ is a scaling and $t()$ a translation function from $\mathbb{R}^D \mapsto \mathbb{R}^{D-d}$, using neural networks.

3 Methodology

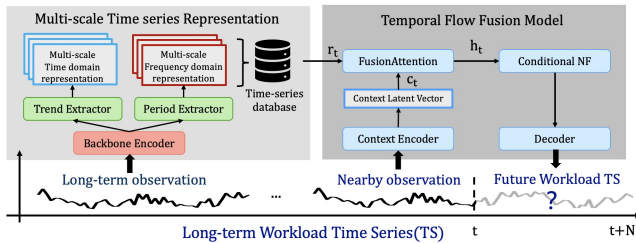


Figure 1: Framework Architecture.

Due to the high-frequency and non-stationary nature of the long-term time series (TS), along with their complex long temporal dependencies spanning daily, weekly, monthly, and quarterly periodicities, it becomes challenging to memorize historical data and learn these dependencies for backcasting. In light of this, we propose a method for representing complex historical TS as compressed vectors and storing them in a TS database. To achieve accurate predictions, we design a *Temporal Flow Fusion Model* that integrates these long-term historical TS representations with near-term observations from nearby windows.

3.1 Multiscale Time Series (TS) Representation

Given TS $y \in \mathbb{R}^{T \times F}$ with backcast window h , our goal is to learn a non-linear embedding function f_θ that maps $\{y_{t-h} \dots y_t\}$ to its representation $r_t = [r_t^T, r_t^F]$, where $r_t \in \mathbb{R}^K$ is for each time stamp t , $r_t^T \in \mathbb{R}^{K_T}$ is the time domain representation, $r_t^F \in \mathbb{R}^{K_F}$ denotes that of frequency domain and $K = K_T + K_F$ is the dimension of representation vectors. In the encoding representation stage, by using backcast windows of various lengths, we can obtain a representation of different scales.

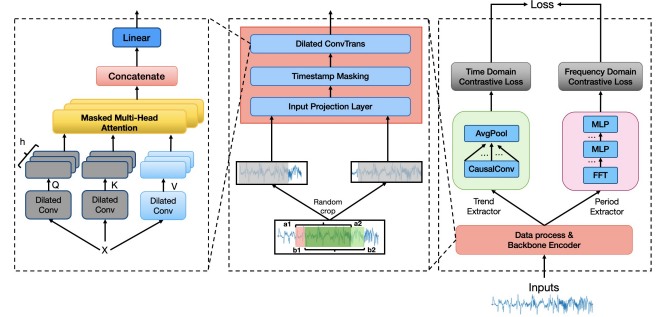


Figure 2: Multiscale Time Series Representation

In Figure 2, we can observe the generation of representation using a schematic view. This process initiates with the random sampling of two overlapping subseries from the input time series, which is then followed by individual data augmentation for each subseries. Subsequently, for the input projection layer, we employ Multilayer Perceptron (MLP), and the original input y_t is mapped into a high-dimensional latent vector z_t . To generate an augmented context view, we employ timestamp masking to mask latent vectors at randomly selected timestamps. The contextual embeddings at each timestamp are then extracted using the ConvTrans backbone encoder. We further extract trends in the time domain and periods in the frequency domain using CausalConv and Fast Fourier transform (FFT), respectively, from the contextual embeddings. In the end, we carry out contrastive learning in both the time and frequency domains.

In the subsequent sections, we provide a detailed description of each of these components.

Random Cropping is a popular data augmentation technique used in contrastive learning for generating new context views. We can randomly sample two overlapping time segments $[a_1, a_2]$ and $[b_1, b_2]$ from TS $y \in \mathbb{R}^{T \times F}$ that satisfy $0 < a_1 < b_1 < a_2 < b_2 \leq T$. Note that contextual representations on the overlapped segment $[b_1, a_2]$ ensure consistency for two context views.

Timestamp Masking aims to produce an augmented context view by randomly masking the timestamps of a TS. We can mask off the latent vector $z = \{z_t\}$ after the Input Projection Layer along the time axis with a binary mask $m \in \{0, 1\}^T$, the elements of which are independently sampled from a Bernoulli distribution with $p = 0.5$.

Backbone Encoder is used to extract the contextual representation at each timestamp. Our selected Backbone Encoder is the 1-layer causal convolution Transformer (ConvTrans), which leverages convolutional multi-head self-attention to capture long- and short-term dependencies.

Specifically, given TS $y \in \mathbb{R}^{T \times F}$, ConvTrans transforms y (as input) into dimension l via dilated causal convolution layer as follows:

$$Q = \text{DilatedConv}(y)$$

$$K = \text{DilatedConv}(y),$$

$$V = \text{DilatedConv}(y)$$

where $Q \in \mathbb{R}^{dl \times dh}$, $K \in \mathbb{R}^{dl \times dh}$, and $V \in \mathbb{R}^{dl \times dh}$ (we denote the length of time steps as dh). After these transformations, the scaled dot-product attention computes the sequence of vector outputs via:

$$S = \text{Attention}(Q, K, V) = \text{softmax}\left(QK^T / \sqrt{d_K} \cdot M\right) V,$$

where the mask matrix M can be applied to filter out right-ward attention (or future information leakage) by setting its upper-triangular elements to $-\infty$ and normalization factor d_K is the dimension of W_h^K matrix. Finally, all outputs S are concatenated and linearly projected again into the next layer. After the above series of operations, we use this backbone f_θ to extract the contextual embedding (intermediate representations) at each timestamp as $\tilde{r} = f_\theta(y)$.

Time Domain Contrastive Learning. A straightforward approach for extracting the underlying trend of a time series (TS) is to employ a collection of 1d causal convolution layers (CasualConv) with varying kernel sizes, along with an average-pooling operation to generate the representations, as shown below:

$$\tilde{r}^{(T,i)} = \text{CausalConv}(\tilde{r}, 2^i)$$

$$r^T = \text{AvgPool}(\tilde{r}^{(T,1)}, \tilde{r}^{(T,2)}, \dots, \tilde{r}^{(T,L)}),$$

where L is a hyper-parameter denoting the number of CasualConv, 2^i ($i = 0, \dots, L$) is the kernel size of each CasualConv, \tilde{r} is above intermediate representations from the backbone encoder, followed by average-pool over the L representations to obtain time-domain representation $\tilde{r}^{(T)}$. To learn discriminative representations over time, we use the time domain contrastive loss, which takes the representations at the same timestamp from two views of the input TS as positive samples ($r_{i,t}^T, \hat{r}_{i,t}^T$), while those at different timestamps from the same time series as negative samples, formulated as

$$\mathcal{L}_{time} = -\log \frac{\exp(r_{i,t}^T \cdot \hat{r}_{i,t}^T)}{\sum_{t' \in \mathcal{T}} (\exp(r_{i,t}^T \cdot \hat{r}_{i,t'}^T) + \mathbb{I}(t \neq t') \exp(r_{i,t}^T \cdot r_{i,t'}^T))}$$

, where \mathcal{T} is the set of timestamps within the overlap of the two subseries, subscript i is the index of the input TS sample, and t is the timestamp.

Frequency Domain Contrastive Learning. Since spectral analysis has proven to be effective in detecting periods, we utilize Fast Fourier Transforms (FFT) to convert the intermediate representations mentioned above to the frequency domain. This allows us to identify various periodic patterns. By combining the FFT and MLP techniques, we can create a period extractor that extracts the frequency spectrum from the contextual embedding and translates it into the freq-based representation r_t^F .

We implement the frequency domain contrastive loss with an index of (i, t) across the batch instances to train the representations to distinguish between various periodic patterns. The formula for this loss is as follows:

$$\mathcal{L}_{freq} = -\log \frac{\exp(r_{i,t}^F \cdot \hat{r}_{i,t}^F)}{\sum_{j \in \mathcal{D}} (\exp(r_{i,t}^F \cdot \hat{r}_{i,t'}^F) + \mathbb{I}(i \neq j) \exp(r_{i,t}^F \cdot r_{i,t'}^F))}$$

, where \mathcal{D} is defined as a batch of TS. We use freq-based representations of other TS at timestamp t in the same batch as negative samples.

The contrastive loss is composed of two losses that are complementary to each other and is defined as

$$\mathcal{L} = \frac{1}{|\mathcal{D}|T} (\mathcal{L}_{time} + \mathcal{L}_{freq}), \quad (3)$$

where \mathcal{D} denotes a batch of TS. As previously noted, we pre-train our TS representation model. **During the encoding representation phase, we use backcast windows of varying lengths to produce representations at different scales.** In this study, we apply this method to encode high-frequency TS data to generate long-term historical TS representations at daily, weekly, monthly, and quarterly intervals.

3.2 Temporal Flow Fusion Model

In this section, we will provide a detailed overview of the *Temporal Flow Fusion Model*. The values of TS will be denoted as $y_t \in \mathbb{R}$, where t represents the time index within the horizon of $t \in 1, 2, \dots, T$. It should be noted that we define x_t as covariates that are known in the future, such as time features and ID features, at time step t .

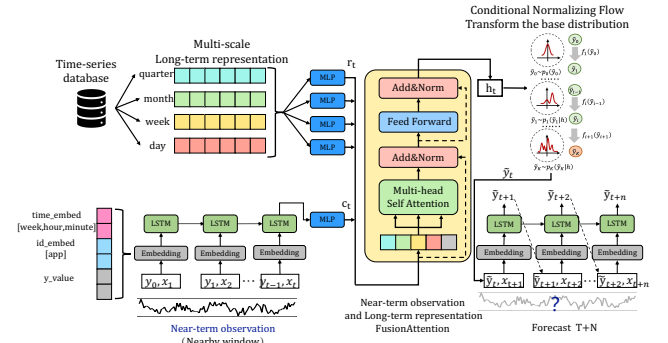


Figure 3: Temporal Flow Fusion Model Architecture.

Given the last L observations y_{t-L}, \dots, y_t , the TS forecasting task aims to predict the future N observations y_{t+1}, \dots, y_{t+N} . We use r_t , the representation of the long-term historical TS, and h_t as the context latent vector from near-term observations (nearby window), to predict future observations. Specifically, our Temporal Flow Fusion Model is structured into three steps, as follows:

First, loading the TS representation and extracting near-term observation features. To begin, we load the Multiscale TS representation r_t from the TS database, which includes daily, weekly, monthly, and quarterly representations. These representations capture various periods and complex long-term temporal dependencies. Next, we apply Recurrent Neural Networks (RNN) to encode short-term observations (within a near-term window) into a context latent vector c_t following Equation 4. This vector captures the nearby window changing pattern of long-term time series data.

$$c_t = \text{RNN}(y_{t-L:t}, x_{t-L:t}; \Theta), \quad (4)$$

where Θ is the learnable parameters of the RNN.

Second, fusing the long-term representation with the near-term observation. After integrating the Multiscale TS representations r_t and the context latent vector c_t into the same dimension using MLP, we construct the FusionAttention employing a multi-head self-attention module, inspired by the transformer architecture, to fuse the long-term historical TS representations and the near-term observations within the nearby window. This fusion module enhances our ability to make accurate predictions by capturing both long-term dependencies and short-term changes within a day.

$$\mathbf{h}_t = \text{FusionAttention}(\mathbf{c}_t, \mathbf{r}_t; \Phi), \quad (5)$$

where Φ is the learnable parameters of the FusionAttention.

Third, employing conditional NF to generate the distribution of the future TS and make predictions. Ultimately, we employ the conditional normalizing flow to approximate the probability density of the TS data. Subsequently, we utilize an RNN as the decoder to facilitate autoregressive decoding and accomplish multi-step prediction.

To estimate the probability density of data (in order to obtain a probabilistic forecast), one straightforward method is to use parameterized Gaussian distribution, but as mentioned above, the real-world hierarchical TS data are mostly non-Gaussian/non-linear. Equipped with the powerful density approximator, NF, we are able to tackle this challenge, capturing the nonlinear relationships among the TS data.

Note that we extend the traditional normalizing flow (NF) to a conditional normalizing flow (CNF). Specifically, we still adopt the Real-NVP architecture, but we extend Equation 2 by concatenating condition \mathbf{h}_t to both the inputs of the scaling and translation function approximators of the coupling layers as follows:

It should be noted that we expand the conventional normalizing flow to a conditional normalizing flow. More specifically, we maintain the Real-NVP architecture while augmenting Equation 2 through the concatenation of condition \mathbf{h}_t to the inputs of the scaling and translation function approximators of the coupling layers, as following below:

$$\begin{cases} \mathbf{y}^{1:d} = \mathbf{z}^{1:d} \\ \mathbf{y}^{d+1:D} = \mathbf{z}^{d+1:D} \odot \exp(s(\mathbf{z}^{1:d}, \mathbf{h}) + t(\mathbf{z}^{1:d}, \mathbf{h})) \end{cases}, \quad (6)$$

where \mathbf{z} is a noise vector sampled from an isotropic Gaussian, functions s (scale) and t (translation) are usually deep neural networks, which as mentioned above, do not need to be invertible.

To obtain an expressive distribution representation, we can stack K layers of conditional flow modules (Real-NVP), generating the conditional distribution of the future sequences of all TS, given the past time $t \in [t-L, t)$. Specifically, it can be written as a product of factors (as an autoregressive model):

$$p(\tilde{\mathbf{y}}_{t:T} | \mathbf{y}_{t-L:t}, \mathbf{x}_{t-L:t}; \theta, \phi, \psi) = \prod_{t=t+1}^T p(\tilde{\mathbf{y}}_t | \mathbf{h}_t; \Psi), \quad (7)$$

where $\tilde{\mathbf{y}}_t$ is the future predictions and Ψ is the parameter of conditional NF.

In the training, given \mathcal{D} , defined as a batch of TS $Y := \{y_1, y_2, \dots, y_T\}$, the representation of the long-term historical TS as r_t , and the associated covariates $X := \{x_1, x_2, \dots, x_T\}$, we can derive the likelihood

as:

$$\mathcal{L} = \frac{1}{|\mathcal{D}|T} \prod_{x_{1:T}, y_{1:T} \in \mathcal{D}} \prod_{t=1}^T p(y_t | y_{1:t}; x_{1:t}, r_t, \Theta, \Phi, \Psi), \quad (8)$$

where Θ is the learnable parameters of the RNN and Φ is the parameter of FusionAttention, and ψ is the parameter of conditional NF.

4 Experiments

We conduct extensive experiments to evaluate the performance of our method on long-term forecasting including 9 real-world benchmarks including 8 well-known datasets in time series and a large real-world workload dataset (RPS data of 1589 microservices from Alipay). Furthermore, We have conducted thorough comparisons with 10 well-acknowledged and advanced baselines.

4.1 Benchmarks

For long-term forecasting, we conduct the experiments on 9 well-established benchmarks: ETT datasets (including 4 subsets: ETTh1, ETTh2, ETTm1, ETTm2) [54], Solar-Energy[24], Weather, Electricity, and Traffic [46], as well as the large Service-Workload datasets.

4.2 Baselines

We compared our method with 10 advanced baselines. These methods can be divided into two categories: end-to-end forecasting models (including PatchTST [31], FEDformer [55], Non-stationary Transformer [26], Autoformer [46], Informer [54]) and time series representation models (including TimeMAE [9], LaST [44], TST[51], COST [45], TS2VEC [50]). Regarding metrics, we utilize the mean square error (MSE) and mean absolute error (MAE) for long-term forecasting.

$$\text{MSE} = \left(\sum_{i=1}^F (\mathbf{X}_i - \hat{\mathbf{X}}_i)^2 \right)^{\frac{1}{2}}, \quad \text{MAE} = \sum_{i=1}^F |\mathbf{X}_i - \hat{\mathbf{X}}_i|,$$

where s is the periodicity of the data. $\mathbf{X}, \hat{\mathbf{X}} \in \mathbb{R}^{F \times C}$ are the ground truth and prediction results of the future with F time points and C dimensions. \mathbf{X}_i means the i -th future time point.

4.3 Main Results

As shown in Table 1, our method achieves consistent state-of-the-art performance across all 9 benchmarks, outperforming 10 advanced baselines. Particularly noteworthy is that compared to the second-best method, our approach achieved a 14% increase in Electricity, 32% in Solar-Energy, 18% in Traffic, and 26% in Workload datasets, highlighting the superiority of our method on complex datasets. Furthermore, we achieved the best performance even on datasets with low forecastability such as ETT and Solar-Energy datasets. We also calculated the standard deviation and conducted statistical significance tests on all datasets in Table 2, and achieved the best performance with a confidence level of over 95% (over 99% in most cases).

Table 1: Long-term forecasting results on 9 benchmarks. All the results are averaged from 4 different prediction lengths, that is {96, 192, 336, 720}. A lower MSE or MAE indicates a better prediction.

Models	Ours (2023)	TimeMAE 2023	TST 2021	LaST 2022	COST 2022	TS2VEC 2022	PatchTST 2023	FEDformer 2022	Stationary 2022	Autoformer 2021	Informer 2020
Metric	MSE MAE	MSE MAE	MSE MAE	MSE MAE	MSE MAE	MSE MAE	MSE MAE	MSE MAE	MSE MAE	MSE MAE	MSE MAE
Weather	0.227 0.263	0.230 0.265	0.239 0.276	0.232 0.261	0.324 0.329	0.233 0.267	0.275 0.280	0.309 0.360	0.288 0.314	0.338 0.382	0.634 0.548
Electricity	0.160 0.255	0.205 0.296	0.209 0.289	0.186 0.274	0.215 0.295	0.213 0.293	0.216 0.318	0.207 0.321	0.213 0.327	0.227 0.338	0.311 0.397
Solar-Energy	0.198 0.252	0.291 0.308	0.294 0.310	0.301 0.332	0.320 0.328	0.369 0.361	0.329 0.400	0.243 0.350	0.340 0.380	0.593 0.557	0.231 0.273
Traffic	0.391 0.272	0.475 0.310	0.586 0.362	0.713 0.397	0.435 0.362	0.470 0.350	0.488 0.327	0.609 0.376	0.624 0.340	0.628 0.379	0.764 0.415
Workload	0.301 0.290	0.405 0.404	0.533 0.515	0.722 0.675	0.683 0.611	0.552 0.513	0.591 0.517	0.609 0.536	0.532 0.550	0.557 0.561	0.564 0.553
ETTh1	0.401 0.425	0.423 0.446	0.466 0.462	0.474 0.461	0.485 0.472	0.446 0.456	0.455 0.444	0.440 0.460	0.57 0.536	0.496 0.487	0.840 0.795
ETTh2	0.328 0.391	0.380 0.386	0.404 0.421	0.499 0.497	0.399 0.427	0.417 0.468	0.384 0.406	0.433 0.447	0.526 0.516	0.453 0.462	4.431 1.729
ETTh1	0.332 0.380	0.366 0.391	0.373 0.389	0.398 0.398	0.356 0.385	0.699 0.557	0.395 0.408	0.448 0.452	0.481 0.456	0.588 0.517	0.961 0.733
ETTh2	0.240 0.319	0.264 0.320	0.297 0.347	0.255 0.326	0.314 0.365	0.326 0.361	0.283 0.327	0.304 0.349	0.306 0.347	0.324 0.368	1.410 0.823

Table 2: Standard deviation and statistical tests for our method and second-best method (TimeMAE) on all benchmarks. We repeat each experiment three times with different random seeds.

Model Dataset	Ours MSE MAE	TimeMAE MSE MAE	Confidence interval
Weather	0.010 0.009	0.012 0.011	99%
Solar-Energy	0.031 0.022	0.020 0.018	99%
Electricity	0.017 0.006	0.012 0.015	95%
Traffic	0.015 0.013	0.008 0.002	99%
workload	0.021 0.023	0.038 0.032	99%
ETTh1	0.022 0.025	0.031 0.051	95%
ETTh2	0.018 0.017	0.015 0.023	99%
ETTh1	0.033 0.016	0.002 0.029	99%
ETTh2	0.021 0.043	0.032 0.022	95%

4.4 Model Analysis

Ablations. To confirm the effectiveness of each component in our approach, we conducted detailed ablations on every possible design within the Multiscale TS representation, FusionAttention, and Conditional NF modules. The following findings can be observed from Table 3 above:

Table 3: Ablations on each component in predict 96-720 set of ETTh1.

Predict Length Components	92	192	336	720
Ours	0.297	0.340	0.343	0.348
W/O Multiscale Repr	0.298	0.350	0.367	0.430
W/O FusionAttention	0.301	0.360	0.368	0.432
W/O Conditional NF	0.296	0.350	0.355	0.415

- The exclusion of the Multiscale TS representation module during the ablation study resulted in a notable decline in performance for longer prediction horizons, particularly for prediction horizons of 336 and 720. This finding shows the effectiveness of our proposed method for representing long-term historical information in time series, precisely the essential multi-periodic and long-term dependent characteristics

inherent in long-term histories that are crucial for accurate long-term forecasting.

- The exclusion of the FusionAttention module led to a reduction in performance for all prediction horizons, underscoring the critical role of properly fusing long-term representations and near-term observations. The findings indicate that accurate long-term forecasting cannot be achieved without an appropriate fusion mechanism, even with long-term historical representations.
- The exclusion of the Conditional NF module decreased the performance, emphasizing the crucial challenge posed by the widespread non-Gaussian/non-linear characteristics present in time series forecasting. This effect was particularly evident in the ablation study, where the performance degradation became more pronounced with an increase in prediction length. These findings highlight the significance of characterizing non-Gaussian/non-linear to achieve accurate long-term forecasting.

Representation analysis. In order to facilitate a better analysis of the Multiscale TS representation, we employ visualizations to provide an intuitive understanding of the TS representation. As seen in Figure 4, our TS representation successfully characterizes long-term temporal dependencies across different periods. We can intuitively see the dependencies between the weekly periods from the representation. Moreover, the TS representation also mines complex nested periods, e.g., the weekly period contains the daily period as shown in the figure. In Figure 4, we plot the visualization of the workload TS representations of different windows, and we can intuitively observe the changes in periods and trends from these representations. Even for TS which does not possess any observable periodic characteristic, our representation can still reveal its corresponding pattern of variations. This attests to the efficacy of our TS representation in capturing long-term temporal dependencies across time periods. Furthermore, we conducted a visual analysis of the clustering of representations, as shown in Figure 5. We can observe that our representations are capable of distinguishing different types of time series in detail. This is evident in both

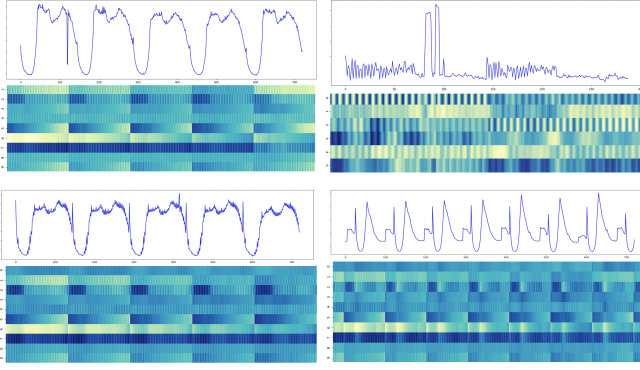


Figure 4: Visualization of TS representation of different windows in Workload TS.

the two-dimensional and three-dimensional clustering visualizations, which demonstrate the effectiveness of our multiscale TS representation.

Forecast results showcases. To evaluate the prediction of different models, we plot the last dimension of forecasting results that are from the test set of the workload TS dataset for qualitative comparison in Figure 6. Among the various models, our method exhibits superior performance.

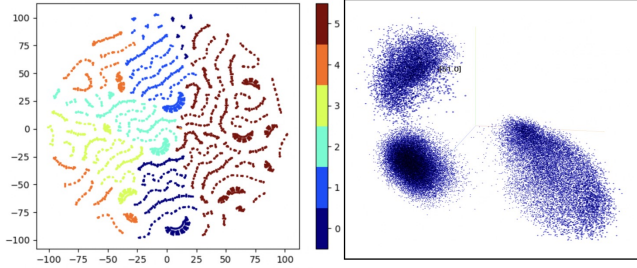


Figure 5: Visualization the clusters of Workload TS representation.

5 Application

Alipay, a leading global mobile payment company, has established its presence in various domains including digital life and digital finance [10]. With an expansive cloud computing infrastructure supporting countless microservices, efficient allocation of cloud resources is critical for Alipay’s cluster management. Alipay relies on its proprietary predictive autoscaling technology as the fundamental component of its cloud resource management system. The accurate prediction of future workloads for each microservice, specifically in terms of requests per second (RPS), is crucial for the effective scaling of server resources. Presently, our proposed approach has been extensively deployed in Alipay’s production cloud environment, achieving remarkable results. The outcomes, as demonstrated in Table 1, indicate a significant improvement of 26% in comparison to the state-of-the-art (SOTA) methods in the real-world environment. It demonstrates the utilization of our autoscaling method based on workload forecasting, which enables the Alipay cloud resource management system to anticipate changes in future workloads through long-term forecasting when traffic

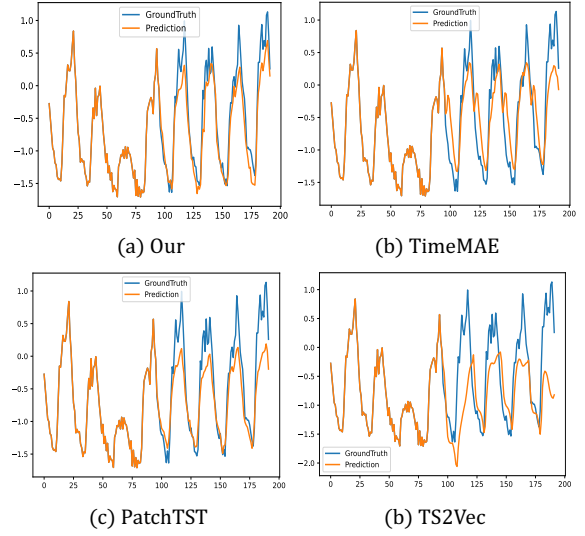


Figure 6: Prediction cases from workload dataset by different models under the input-96-predict-96 settings.

fluctuates. This facilitates the scaling of computing resources to allocate those appropriate for the current workload. Upon activating our prediction technique, the number of pods (containers that host microservices) utilized by the microservices has significantly decreased from 1500 to less than 500 (Reduced resource consumption by 67%), leading to a substantial improvement in resource utilization efficiency.

6 Conclusion

This paper presents a novel framework for accurate long-term workload forecasting by incorporating a multiscale time series representation method and a temporal flow fusion model. The framework uniquely captures both long-term historical patterns and near-term observations in the workload time series for superior predictions. To our knowledge, this is the first deep integration of multiscale representation learning and deep forecast modeling for time series. Comprehensive evaluations on 9 benchmarks demonstrate consistent state-of-the-art performance over 10 advanced baselines. Furthermore, when deployed on a real-world cloud resource management system with over a thousand sets of microservices, significant improvements in scheduling and resource management are achieved. This end-to-end framework successfully leverages multiscale representations and temporal fusion to advance the capability of AI systems for long-term time series forecasting.

References

- [1] George EP Box and Gwilym M Jenkins. 1968. Some recent advances in forecasting and control. *Journal of the Royal Statistical Society. Series C (Applied Statistics)* 17, 2 (1968), 91–109.
- [2] Serafeim Chatzopoulos, Thanasis Vergoulis, Dimitrios Skoutas, Theodore Dalamagas, Christos Tryfonopoulos, and Panagiotis Karras. 2023. Atrapos: Real-time Evaluation of Metapath Query Workloads. In *Proceedings of the ACM Web Conference 2023*. 2487–2498.
- [3] Ting Chen, Simon Kornblith, Mohammad Norouzi, and Geoffrey Hinton. 2020. A simple framework for contrastive learning of visual representations. In *International conference on machine learning*. PMLR, 1597–1607.
- [4] Ting Chen, Simon Kornblith, Kevin Swersky, Mohammad Norouzi, and Geoffrey E Hinton. 2020. Big self-supervised models are strong semi-supervised learners.

- Advances in neural information processing systems* 33 (2020), 22243–22255.
- [5] Xinlei Chen, Haoqi Fan, Ross Girshick, and Kaiming He. 2020. Improved baselines with momentum contrastive learning. *arXiv preprint arXiv:2003.04297* (2020).
 - [6] Xinlei Chen and Kaiming He. 2021. Exploring simple siamese representation learning. In *Proceedings of the IEEE/CVF conference on computer vision and pattern recognition*. 15750–15758.
 - [7] Xinlei Chen*, Saining Xie*, and Kaiming He. 2021. An Empirical Study of Training Self-Supervised Vision Transformers. *arXiv preprint arXiv:2104.02057* (2021).
 - [8] Zhichao Chen, Leilei Ding, Zhixuan Chu, Yucheng Qi, Jianmin Huang, and Hao Wang. 2023. Monotonic neural ordinary differential equation: Time-series forecasting for cumulative data. In *Proceedings of the 32nd ACM International Conference on Information and Knowledge Management*. 4523–4529.
 - [9] Mingyue Cheng, Qi Liu, Zhiding Liu, Hao Zhang, Rujiao Zhang, and Enhong Chen. 2023. TimeMAE: Self-Supervised Representations of Time Series with Decoupled Masked Autoencoders. *TKDE* (2023).
 - [10] Zhixuan Chu, Hui Ding, Guang Zeng, Yuchen Huang, Tan Yan, Yulin Kang, and Sheng Li. 2022. Hierarchical capsule prediction network for marketing campaigns effect. In *Proceedings of the 31st ACM International Conference on Information & Knowledge Management*. 3043–3051.
 - [11] Zhixuan Chu, Mengxuan Hu, Qing Cui, Longfei Li, and Sheng Li. 2024. Task-driven causal feature distillation: Towards trustworthy risk prediction. In *Proceedings of the AAAI Conference on Artificial Intelligence*, Vol. 38. 11642–11650.
 - [12] Shohreh Deldari, Daniel V Smith, Hao Xue, and Flora D Salim. 2021. Time series change point detection with self-supervised contrastive predictive coding. In *Proceedings of the Web Conference 2021*. 3124–3135.
 - [13] Fan Deng, Jie Lu, Shi-Yu Wang, Jie Pan, and Li-Yong Zhang. 2019. A distributed PDP model based on spectral clustering for improving evaluation performance. *World Wide Web* 22 (2019), 1555–1576.
 - [14] Fan Deng, Shiyu Wang, Liyong Zhang, Xiaoqian Wei, and Jingping Yu. 2018. Establishment of attribute bitmaps for efficient XACML policy evaluation. *Knowledge-Based Systems* 143 (2018), 93–101.
 - [15] Laurent Dinh, Jascha Sohl-Dickstein, and Samy Bengio. 2017. Density estimation using Real NVP. *arXiv:1605.08803* [cs.LG]
 - [16] Emadeldeen Eldele, Mohamed Ragab, Zhenghua Chen, Min Wu, Chee Keong Kwah, Xiaoli Li, and Cuntai Guan. 2021. Time-series representation learning via temporal and contextual contrasting. *arXiv preprint arXiv:2106.14112* (2021).
 - [17] Binbin Feng and Zhijun Ding. 2023. GROUP: An End-to-end Multi-step-ahead Workload Prediction Approach Focusing on Workload Group Behavior. In *Proceedings of the ACM Web Conference 2023*. 3098–3108.
 - [18] Kaiming He, Haoqi Fan, Yuxin Wu, Saining Xie, and Ross Girshick. 2020. Momentum contrast for unsupervised visual representation learning. In *Proceedings of the IEEE/CVF conference on computer vision and pattern recognition*. 9729–9738.
 - [19] Min Hou, Chang Xu, Yang Liu, Weiqing Liu, Jiang Bian, Le Wu, Zhi Li, Enhong Chen, and Tie-Yan Liu. 2021. Stock trend prediction with multi-granularity data: A contrastive learning approach with adaptive fusion. In *Proceedings of the 30th ACM International Conference on Information & Knowledge Management*. 700–709.
 - [20] Qin Hua, Dingyu Yang, Shiyu Qian, Hanwen Hu, Jian Cao, and Guangtao Xue. 2023. KAE-Informer: A Knowledge Auto-Embedding Informer for Forecasting Long-Term Workloads of Microservices. In *Proceedings of the ACM Web Conference 2023*. 1551–1561.
 - [21] Ming Jin, Shiyu Wang, Lintao Ma, Zhixuan Chu, James Y Zhang, Xiaoming Shi, Pin-Yu Chen, Yuxuan Liang, Yuan-Fang Li, Shirui Pan, and Qingsong Wen. 2024. Time-LLM: Time series forecasting by reprogramming large language models. In *International Conference on Learning Representations (ICLR)*.
 - [22] Diederik P Kingma and Max Welling. 2013. Auto-encoding variational bayes. *arXiv preprint arXiv:1312.6114* (2013).
 - [23] Ivan Kobyzev, Simon Prince, and Marcus Brubaker. 2020. Normalizing flows: An introduction and review of current methods. *IEEE Transactions on Pattern Analysis and Machine Intelligence* (2020).
 - [24] Guokun Lai, Wei-Cheng Chang, Yiming Yang, and Hanxiao Liu. 2018. Modeling Long- and Short-Term Temporal Patterns with Deep Neural Networks. *arXiv:1703.07015* [cs.LG]
 - [25] Yanan Li, Haitao Yuan, Zhe Fu, Xiao Ma, Mengwei Xu, and Shangguang Wang. 2023. ELASTIC: Edge Workload Forecasting based on Collaborative Cloud-Edge Deep Learning. In *Proceedings of the ACM Web Conference 2023*. 3056–3066.
 - [26] et al Liu, Yong. 2022. Non-stationary transformers: Exploring the stationarity in time series forecasting. *Advances in Neural Information Processing Systems* 35 (2022), 9881–9893.
 - [27] Yong Liu, Tengge Hu, Haoran Zhang, Haixu Wu, Shiyu Wang, Lintao Ma, and Mingsheng Long. 2023. itransformer: Inverted transformers are effective for time series forecasting. *arXiv preprint arXiv:2310.06625* (2023).
 - [28] Spyros Makridakis and Michele Hibon. 1997. ARMA models and the Box-Jenkins methodology. *Journal of forecasting* 16, 3 (1997), 147–163.
 - [29] Mohammad Masdari and Afsane Khoshnevis. 2020. A survey and classification of the workload forecasting methods in cloud computing. *Cluster Computing* 23, 4 (2020), 2399–2424.
 - [30] Janmenjoy Nayak, Bighnaraj Naik, AK Jena, Rabindra K Barik, and Himansu Das. 2018. Nature inspired optimizations in cloud computing: applications and challenges. *Cloud computing for optimization: Foundations, applications, and challenges* (2018), 1–26.
 - [31] Yuqi Nie, Nam H. Nguyen, Phanwadee Sinthong, and Jayant Kalagnanam. 2023. A Time Series is Worth 64 Words: Long-term Forecasting with Transformers. In *Proceedings of the AAAI Conference on Artificial Intelligence*.
 - [32] George Papamakarios, Eric Nalisnick, Danilo Jimenez Rezende, Shakir Mohamed, and Balaji Lakshminarayanan. 2019. Normalizing flows for probabilistic modeling and inference. *arXiv preprint arXiv:1912.02762* (2019).
 - [33] George Papamakarios, Eric Nalisnick, Danilo Jimenez Rezende, Shakir Mohamed, and Balaji Lakshminarayanan. 2021. Normalizing flows for probabilistic modeling and inference. *The Journal of Machine Learning Research* 22, 1 (2021), 2617–2680.
 - [34] Haoran Qiu, Subho S Banerjee, Saurabh Jha, Zbigniew T Kalbarczyk, and Ravishanker K Iyer. 2020. {FIRM}: An intelligent fine-grained resource management framework for {SLO-Oriented} microservices. In *14th USENIX symposium on operating systems design and implementation (OSDI 20)*. 805–825.
 - [35] Danilo Rezende and Shakir Mohamed. 2015. Variational inference with normalizing flows. In *International conference on machine learning*. PMLR, 1530–1538.
 - [36] Nilabja Roy, Abhishek Dubey, and Aniruddha Gokhale. 2011. Efficient autoscaling in the cloud using predictive models for workload forecasting. In *2011 IEEE 4th International Conference on Cloud Computing*. IEEE, 500–507.
 - [37] Krzysztof Rzadca, Pawel Findeisen, Jacek Swiderski, Przemyslaw Zych, Przemyslaw Broniek, Jarek Kusmierek, Pawel Nowak, Beata Strack, Piotr Witusowski, Steven Hand, et al. 2020. Autopilot: workload autoscaling at Google. In *Proceedings of the Fifteenth European Conference on Computer Systems*. 1–16.
 - [38] David Salinas, Valentin Flunkert, Jan Gasthaus, and Tim Januschowski. 2020. DeepAR: Probabilistic forecasting with autoregressive recurrent networks. *International Journal of Forecasting* 36, 3 (2020), 1181–1191.
 - [39] Shiyu Wang. 2024. NeuralReconciler for Hierarchical Time Series Forecasting. In *Proceedings of the 17th ACM International Conference on Web Search and Data Mining*. 731–739.
 - [40] Shiyu Wang, Yinbo Sun, Xiaoming Shi, Shiyi Zhu, Lin-Tao Ma, James Zhang, Yifei Zheng, and Jian Liu. 2023. Full scaling automation for sustainable development of green data centers. *arXiv preprint arXiv:2305.00706* (2023).
 - [41] Shiyu Wang, Yinbo Sun, Yan Wang, Lin-Tao Ma, James Zhang, and Yangfei Zheng. 2023. Flow-Based End-to-End Model for Hierarchical Time Series Forecasting via Trainable Attentive-Reconciliation. In *International Conference on Database Systems for Advanced Applications*. Springer, 167–176.
 - [42] Shiyu Wang, Haixu Wu, Xiaoming Shi, Tengge Hu, Huakun Luo, Lintao Ma, James Y Zhang, and JUN ZHOU. 2024. TimeMixer: Decomposable Multiscale Mixing for Time Series Forecasting. In *International Conference on Learning Representations (ICLR)*.
 - [43] Shiyu Wang, Fan Zhou, Yinbo Sun, Lintao Ma, James Zhang, and Yangfei Zheng. 2022. End-to-end modeling of hierarchical time series using autoregressive transformer and conditional normalizing flow-based reconciliation. In *2022 IEEE International Conference on Data Mining Workshops (ICDMW)*. IEEE, 1087–1094.
 - [44] Zhiyuan Wang, Xovee Xu, Weifeng Zhang, Goe Trajcevski, Ting Zhong, and Fan Zhou. 2022. Learning latent seasonal-trend representations for time series forecasting. *Advances in Neural Information Processing Systems* 35 (2022), 38775–38787.
 - [45] Gerald Woo, Chenghao Liu, Doyen Sahoo, Akshat Kumar, and Steven Hoi. 2022. CoST: Contrastive learning of disentangled seasonal-trend representations for time series forecasting. *arXiv preprint arXiv:2202.01575* (2022).
 - [46] Haixu Wu, Jiehui Xu, Jianmin Wang, and Mingsheng Long. 2021. Autoformer: Decomposition transformers with auto-correlation for long-term series forecasting. *Advances in Neural Information Processing Systems* 34 (2021), 22419–22430.
 - [47] Siqiao Xue, Xiaoming Shi, Zhixuan Chu, Yan Wang, Fan Zhou, Hongyan Hao, Caigao Jiang, Chen Pan, Yi Xu, James Y Zhang, et al. 2023. Easytpp: Towards open benchmarking the temporal point processes. *arXiv preprint arXiv:2307.08097* (2023).
 - [48] Siqiao Xue, Yan Wang, Zhixuan Chu, Xiaoming Shi, Caigao Jiang, Hongyan Hao, Gangwei Jiang, Xiaoyun Feng, James Zhang, and Jun Zhou. 2023. Prompt-augmented temporal point process for streaming event sequence. *Advances in Neural Information Processing Systems* 36 (2023), 18885–18905.
 - [49] Jianwei Yin, Xingjian Lu, Hanwei Chen, Xinkui Zhao, and Neal N Xiong. 2014. System resource utilization analysis and prediction for cloud based applications under bursty workloads. *Information Sciences* 279 (2014), 338–357.
 - [50] Zhihan Yue, Yujing Wang, Juanyong Duan, Tianmeng Yang, Congrui Huang, Yunhai Tong, and Bixiong Xu. 2022. Ts2vec: Towards universal representation of time series. In *Proceedings of the AAAI Conference on Artificial Intelligence*, Vol. 36. 8980–8987.
 - [51] George Zerveas, Srideepika Jayaraman, Dhaval Patel, Anuradha Bhamidipaty, and Carsten Eickhoff. 2021. A transformer-based framework for multivariate time series representation learning. In *Proceedings of the 27th ACM SIGKDD Conference on Knowledge Discovery & Data Mining*. 2114–2124.

- [52] Kexin Zhang, Qingsong Wen, Chaoli Zhang, Rongyao Cai, Ming Jin, Yong Liu, James Zhang, Yuxuan Liang, Guansong Pang, Dongjin Song, et al. 2023. Self-Supervised Learning for Time Series Analysis: Taxonomy, Progress, and Prospects. *arXiv preprint arXiv:2306.10125* (2023).
- [53] Xiang Zhang, Ziyuan Zhao, Theodoros Tsiligkaridis, and Marinka Zitnik. 2022. Self-supervised contrastive pre-training for time series via time-frequency consistency. *Advances in Neural Information Processing Systems* 35 (2022), 3988–4003.
- [54] Haoyi Zhou, Shanghang Zhang, Jieqi Peng, Shuai Zhang, Jianxin Li, Hui Xiong, and Wancai Zhang. 2021. Informer: Beyond efficient transformer for long sequence time-series forecasting. In *Proceedings of AAAI*.
- [55] Tian Zhou, Ziqing Ma, Qingsong Wen, Xue Wang, Liang Sun, and Rong Jin. 2022. FEDformer: Frequency enhanced decomposed transformer for long-term series forecasting. *arXiv preprint arXiv:2201.12740* (2022).
- [56] Yunyi Zhou, Zhixuan Chu, Yijia Ruan, Ge Jin, Yuchen Huang, and Sheng Li. 2023. ptse: A multi-model ensemble method for probabilistic time series forecasting. *arXiv preprint arXiv:2305.11304* (2023).